

Comparison of cavity structures of 200 MHz repetition rate erbium-doped fiber lasers

Jiawei Liu(刘佳伟), Yuyao Zong(宗玉瑶), Yi Han(韩羿)5, and Shiying Cao(曹士英)
Citation: Chin. Phys. B, 2026, 35 (**6**): 064209. DOI: 10.1088/1674-1056/ae5f86
http://cpb.iphy.ac.cn; http://iopscience.iop.org/cpb

What follows is a list of articles you may be interested in

Generation of wavelength-tunable, bound-state and noise-like pulses in an all-polarization-maintaining laser ring cavity based on nonlinear polarization evolution

Yazhou Shi(石亚洲), Ze Li(李泽), and Zhiguo Lv(吕志国)
Chin. Phys. B, 2026, 35 (**5**): 054202. DOI: 10.1088/1674-1056/ae15f3

Dissipative soliton operation in a mode-locked laser based on thulium-doped fiber

Wen-Yan Zhang(张文艳), Lei Zheng(郑磊), Tian Zhang(张添), Nan-Nan Liu(刘楠楠), Li-Jie Geng(耿利杰), Kun Yang(杨坤), and Li Zhan(詹黎)
Chin. Phys. B, 2026, 35 (**4**): 044201. DOI: 10.1088/1674-1056/ae063c

High-efficiency Yb^{3+}-doped fiber laser with highly optical nonlinear Bi_4Br_4-based saturable absorber

Mengyuan Liu(刘梦媛), Yechao Han(韩烨超), Qi Liu(刘齐), Hao Teng(滕浩), Xiwei Huang(黄玺玮), Xiaowei Xing(邢笑伟), Xiangyu Qiao(乔向宇), Guojing Hu(胡国静), Xiao Lin(林晓), Haitao Yang(杨海涛), Zhiyi Wei(魏志义), and Wenjun Liu(刘文军)
Chin. Phys. B, 2025, 34 (**6**): 064202. DOI: 10.1088/1674-1056/adc664

Pure-quartic soliton molecules in normal fourth-order dispersion regimes based on spectral filtering effect

Han-Yang Shen(申翰阳), Rui-Bo Lan(蓝睿博), Hong-Bin Hu(胡洪彬), Yang Li(李阳), Rui Zhou(周瑞), and Zu-Xing Zhang(张祖兴)
Chin. Phys. B, 2025, 34 (**3**): 034203. DOI: 10.1088/1674-1056/ada43c

Dissipative soliton resonance within different dispersion regimes in a single mode-locked laser

Zhetao Zhao(赵哲韬), Qinke Shu(舒沁珂), Ziyi Xie(解梓怡), Yuxuan Ren(任俞宣), Ying Zhang(张颖), Bo Yuan(袁博), Chunbo Zhao(赵春勃), Junsong Peng(彭俊松), and Heping Zeng(曾和平)
Chin. Phys. B, 2024, 33 (**7**): 074208. DOI: 10.1088/1674-1056/ad47b1

SPECIAL TOPIC — Ultrafast physics in atomic, molecular and optical systems

Comparison of cavity structures of 200 MHz repetition rate erbium-doped fiber lasers

Jiawei Liu(刘佳伟)[1,2,3], Yuyao Zong(宗玉瑶)[4], Yi Han(韩羿)[5], and Shiying Cao(曹士英)[1,2,3,†]

[1] *Division of Time and Frequency Metrology, National Institute of Metrology, Beijing* 100029, *China*
[2] *Key Laboratory of State Administration for Market Regulation, Time Frequency and Gravity Primary Standard, National Institute of Metrology, Beijing* 100029, *China*
[3] *Beijing Key Laboratory of Quantum Metrology Technology and Instruments, National Institute of Metrology, Beijing* 100029, *China*
[4] *College of Information Engineering, China Jiliang University, Hangzhou* 310018, *China*
[5] *State Key Laboratory of Luminescent Materials and Devices, School of Materials Science and Engineering, South China University of Technology, Guangzhou* 510640, *China*

(Received 5 February 2026; revised manuscript received 2 April 2026; accepted manuscript online 15 April 2026)

As an important component of optical frequency combs, mode-locked lasers are also the main source of noise in optical frequency combs. This paper focuses on the effect of the cavity structure of mode-locked lasers on noise performance. At a pump power of 793 mW, the integrated timing jitter within the range of 10 Hz–10 kHz for the ring cavity, σ cavity, and Figure-9 cavity is 216 fs, 307 fs, and 107 fs, respectively, while the integrated relative intensity noise from 1 Hz to 1 MHz is 0.0050%, 0.0029%, and 0.0037%, respectively. The Figure-9 cavity demonstrates superior noise performance, and the σ cavity based on nonlinear polarization rotation also exhibits certain resistance to noise interference.

Keywords: mode-locked fiber laser, laser cavity structure, noise, optical frequency comb

PACS: 42.55.Wd, 42.60.Da, 42.62.Eh

DOI: 10.1088/1674-1056/ae5f86 **CSTR:** 32038.14.CPB.ae5f86

1. Introduction

Narrow-linewidth, low-noise optical frequency combs based on fiber mode-locked lasers have wide applications in fields such as time-frequency measurement,[1] absolute distance measurement,[2] optical clock comparison,[3] time-frequency transfer,[4] dual-comb spectroscopy[5–7] and ultra-stable microwave generation.[8,9] The main noise sources of an optical frequency comb include amplified spontaneous emission noise, temperature fluctuations, vibrations, and pump noise. Extracavity noise mainly appears as white noise, reducing the signal-to-noise ratio and visibility of the comb lines, while intracavity noise primarily manifests as frequency noise, which broadens the comb lines.[10,11] Therefore, a low-noise mode-locked laser is crucial for achieving a low-noise, narrow-linewidth optical frequency comb.

The noise performance of the mode-locked laser is also influenced by factors such as the mode-locking mechanism, dispersion, and cavity structure.[12] In terms of the mode-locking mechanism, artificial saturable absorbers based on nonlinear polarization rotation (NPR) and nonlinear amplifying loop mirrors (NALMs) exhibit lower noise.[13] In terms of dispersion, near-zero dispersion results in lower phase noise.[14–16] To reduce the demands on phase-locked loops and facilitate applications in narrow-linewidth optical combs, it is essential to investigate the impact of cavity structure on laser noise, particularly under conditions of near-zero dispersion and artificial saturable absorber mode-locking.[12]

Many researchers have already shown interest in the inherent noise performance of free-running mode-locked lasers. In 2015, Li *et al.*[17] demonstrated a 201 MHz repetition-rate NPR mode-locked erbium-doped fiber laser in a ring cavity. The 8th harmonic of the repetition rate had a phase noise of approximately −120 dBc/Hz at a 1 kHz offset frequency, and the timing jitter from 1 kHz to 10 MHz was 24 fs. In 2017, Menlo Systems constructed an all-polarization-maintaining Figure-9 cavity erbium-doped fiber laser with a repetition rate of 250 MHz based on the NALM mode-locking mechanism. The laser achieved an integrated relative intensity noise (RIN) better than 0.005% over offset frequencies from 1 Hz to 1 MHz.[18] In 2019, Wang *et al.* built a σ cavity erbium-doped mode-locked fiber laser operating at a repetition rate of 97.6 MHz, based on NPR and a semiconductor saturable absorber mirror (SESAM). The RIN at a 1 Hz offset frequency was approximately −110 dBc/Hz, but quickly decreased to −120 dBc/Hz.[19] For each cavity structure, only one report is presented here; more examples can be found in the references.[20–22]

In this work, we independently constructed a Figure-9

†Corresponding author. E-mail: caoshiying@nim.ac.cn

© 2026 Chinese Physical Society and IOP Publishing Ltd. All rights, including for text and data mining, AI training, and similar technologies, are reserved.

cavity laser based on NALM mode-locking, as well as a ring cavity laser and a σ cavity laser based on NPR mode-locking. To minimize interference from factors other than the cavity structure, the repetition rates of the three lasers were controlled at 200 MHz, their dispersions were kept similar, the pump currents were maintained consistently, and the lasers were placed on a stable optical platform in the laboratory for noise measurements to reduce the environmental sensitivity of non-polarization-maintaining fibers. At a pump power of 793 mW, the integrated timing jitter within the range of 10 Hz–10 kHz for the ring cavity, σ cavity, and Figure-9 cavity was 216 fs, 307 fs, and 107 fs, respectively, while the integrated RIN from 1 Hz to 1 MHz was 0.0050%, 0.0029%, and 0.0037%, respectively.

2. Experimental setup

The fiber mode-locked lasers with different cavity structures are shown in Fig. 1.

To isolate the effect of the cavity structure, all other parameters were kept consistent by ensuring comparable active fiber lengths and net dispersion across the three lasers, thereby mitigating the known impact of dispersion on phase noise.[14–16] The specific fiber lengths and dispersion parameters of each laser are shown in Table 1.

Table 1. Fiber lengths and net dispersion of three different structures of erbium-doped mode-locked lasers.

Cavity structure	Co1	Er	WDM (Common)	WDM (Pass)&Co2	Net dispersion
Ring	SMF28e	Er110	OFS980	OFS980 + SMF28e	
	20 cm	41 cm	8.5 cm	7 + 11 cm	-1621 fs^2
σ	SMF28e	Er110	OFS980	OFS980 + SMF28e	
	10 cm	38 cm	8 cm	7 + 24 cm	-2650 fs^2
Figure-9	PMSMF	Er80	PMSMF	PMSMF	
	7 cm	43 cm	17 cm	10 + 7.7 cm	-574 fs^2

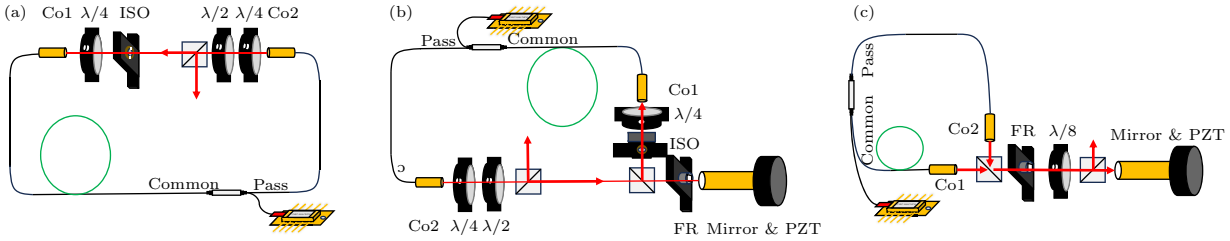


Fig. 1. The cavity structures of erbium-doped fiber mode-locked lasers with a repetition rate of 200 MHz. (a) Ring cavity. (b) σ cavity. (c) Figure-9 cavity.

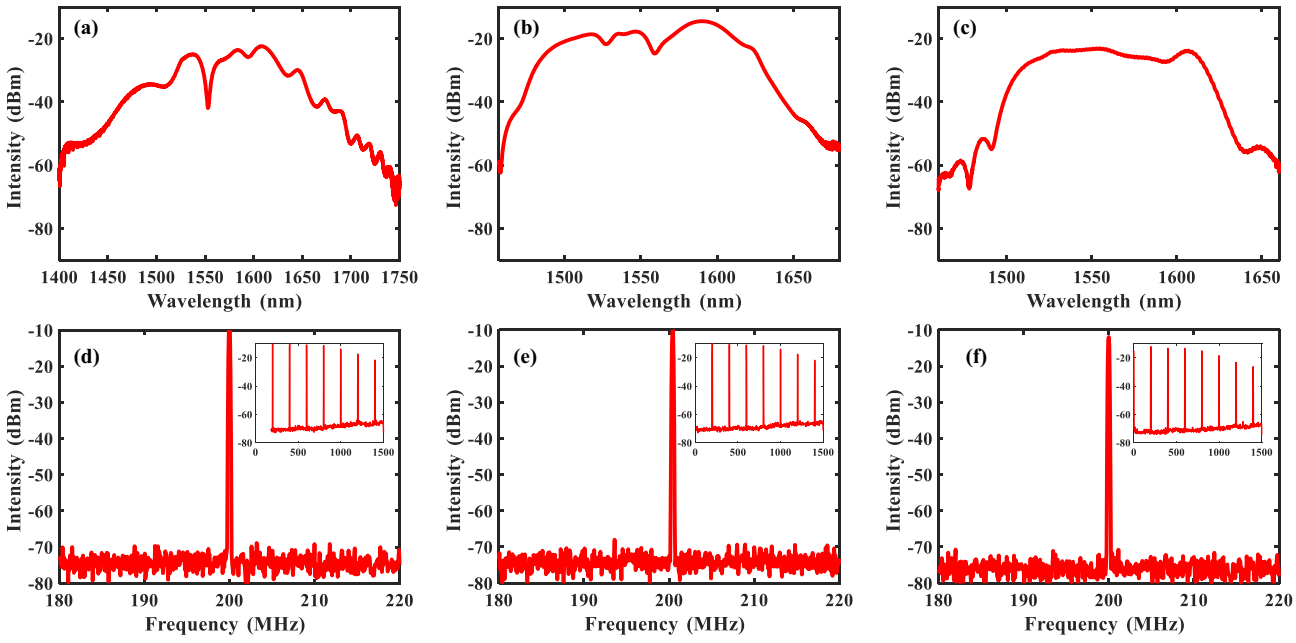


Fig. 2. Optical spectrum (a)–(c) and corresponding radio-frequency spectrum (d)–(f) for the ring, σ, and Figure-9 cavity lasers, respectively.

3. Results

3.1. Basic parameters of three lasers

By optimizing the fiber length, the net cavity dispersion was brought close to zero dispersion, and the repetition rate was controlled to be near 200 MHz. Ultimately, a repetition rate of 200 MHz was achieved. At a pump current of 1100 mA (793 mW), the 3 dB bandwidths for the ring, σ, and Figure-9 cavities were 87 nm, 30 nm, and 92 nm, respectively, while their 5 dB bandwidths were 99 nm, 101 nm, and 103 nm, respectively. The output powers of the three lasers were around 30 mW. The corresponding optical spectra and radio-frequency spectra (span 40 MHz, RBW 100 kHz) are presented in Fig. 2.

3.2. Selection of laser diode drivers

The noise from the laser diode is one of the significant noise sources in fiber-based mode-locked lasers. To minimize the RIN of the laser diode and achieve optimal noise performance for the seed source, we evaluated three commercially available drivers using the same laser diode. When measuring the RIN of the laser diode, the driver current was set to 600 mA, the detector used was the Thorlabs PDA10CS-EC, and the noise analyzer was the Agilent Technologies E5052B. The measurement results are shown in Fig. 3.

In the offset frequency range from 1 Hz to 1 MHz, the integrated RIN of the Thorlabs CLD1015, Thorlabs PRO8000, and Koheron CTL300E were 0.2776%, 0.3028%, and 0.2660%, respectively. Therefore, when measuring the noise of lasers with different cavity structures, we chose the Koheron CTL300E as the driver for the laser diode.

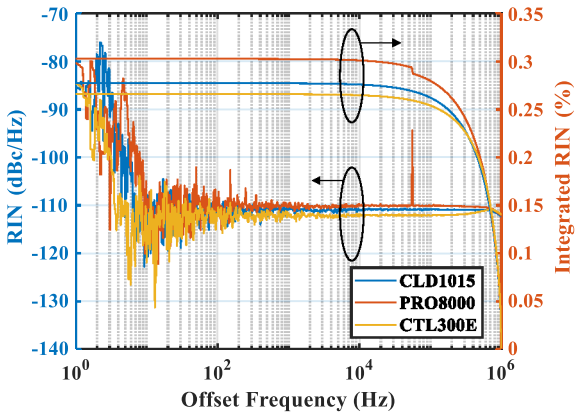


Fig. 3. Laser diode RIN under three laser diode drivers.

3.3. Noise measurement of lasers with different cavity structures

The three lasers were enclosed in simple plastic boxes and placed on the laboratory optical table for noise measurements. The detectors used for phase noise and RIN measurements were EOT ET-5000F and Thorlabs PDA10CS-EC, respectively, and the noise analyzer was an Agilent Technologies E5052B. Under the same laser diode and driven by the Koheron CTL300E, the measured phase noise and RIN are shown in Fig. 4. In Fig. 4(b), we also present the RIN of the laser diode at a pump power of 793 mW (corresponding to 1100 mA).

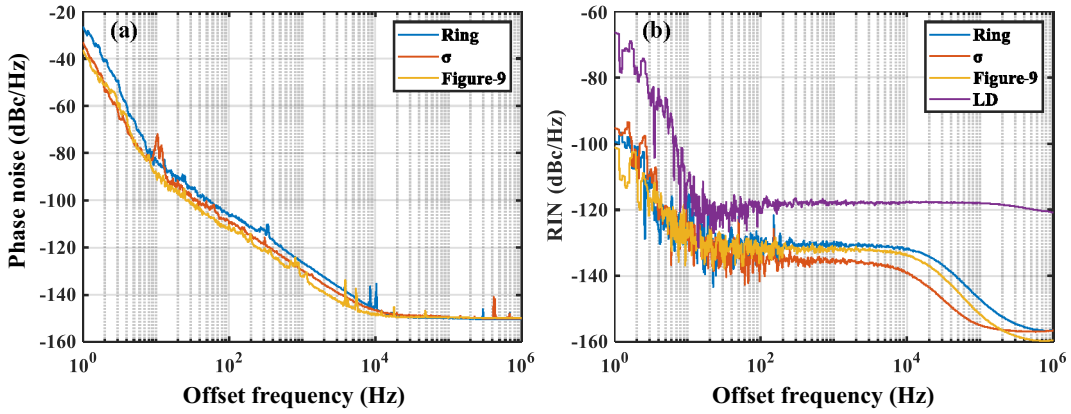


Fig. 4. (a) Phase noise and (b) RIN of fiber mode-locked lasers with different cavity structures.

Table 2. Integrated time jitter of three lasers with different cavity structures.

Offset frequency range	Ring	σ	Figure-9
1 Hz–1 MHz	28844 fs	11144 fs	8220 fs
10 Hz–1 MHz	219 fs	309 fs	113 fs
100 Hz–1 MHz	72 fs	56 fs	48 fs
1000 Hz–1 MHz	39 fs	40 fs	38 fs

The integrated timing jitter of the ring cavity, σ cavity, and Figure-9 cavity over different offset frequency ranges is shown in Table 2. The corresponding integrated RIN from 1 Hz to 1 MHz was 0.0050%, 0.0029%, and 0.0037%, respectively. At offset frequencies below 3 kHz, the Figure-9 cavity outperforms both the σ cavity and the ring cavity. In terms of RIN, the σ cavity outperforms the Figure-9 cavity and the ring cavity. Furthermore, compared with the ring cavity, the σ cavity demonstrates a certain degree of noise resistance.

When analyzing the RIN of fiber amplifiers with the same

doped medium, there exists a pump-to-seed noise transfer function between the output light and the pump light.[15,23,24] This theory can be used to analyze the response of lasers with different cavity structures to laser diode RIN. Unlike amplifiers, the same doped fiber is placed in oscillators with different cavity structures. As shown in Fig. 4(b), the following characteristics are still observed at offset frequencies below 1 kHz. Compared with amplifiers, oscillators exhibit a certain suppression capability for low-frequency RIN, approximately $10 \sim 20$ dB. The coupling of the laser diode mid-frequency RIN to the oscillator manifests as attenuation. Lasers with different cavity structures exhibit different suppression capabilities. From 1 kHz to 10 kHz, the attenuation is relatively slow, and the RIN remains relatively flat on a logarithmic scale. Beyond an offset frequency of 10 kHz, the RIN is suppressed due to the slow relaxation constant of erbium ions.[18]

For phase noise measurements, we used a simple conventional method, namely, a photodetector (EOT ET-5000F) combined with a signal source analyzer (Agilent E5052B). Compared with more state-of-the-art methods, such as the balanced optical cross-correlation (BOC), fiber-delay method, or optical heterodyning method,[15,25,26] this method is limited by detector thermal noise and shot noise at higher offset frequencies. As shown in Fig. 4(a), the phase noise curve becomes flat after 10 kHz. At higher offset frequencies, there is also a contribution from amplified spontaneous emission (ASE) in the gain fiber. From the measurement results, the phase noise of the Figure-9 cavity is lower than that of the σ cavity and the ring cavity. Overall, the Figure-9 cavity demonstrates superior noise performance. Surprisingly, the σ cavity based on NPR mode-locking also demonstrates a degree of noise suppression.

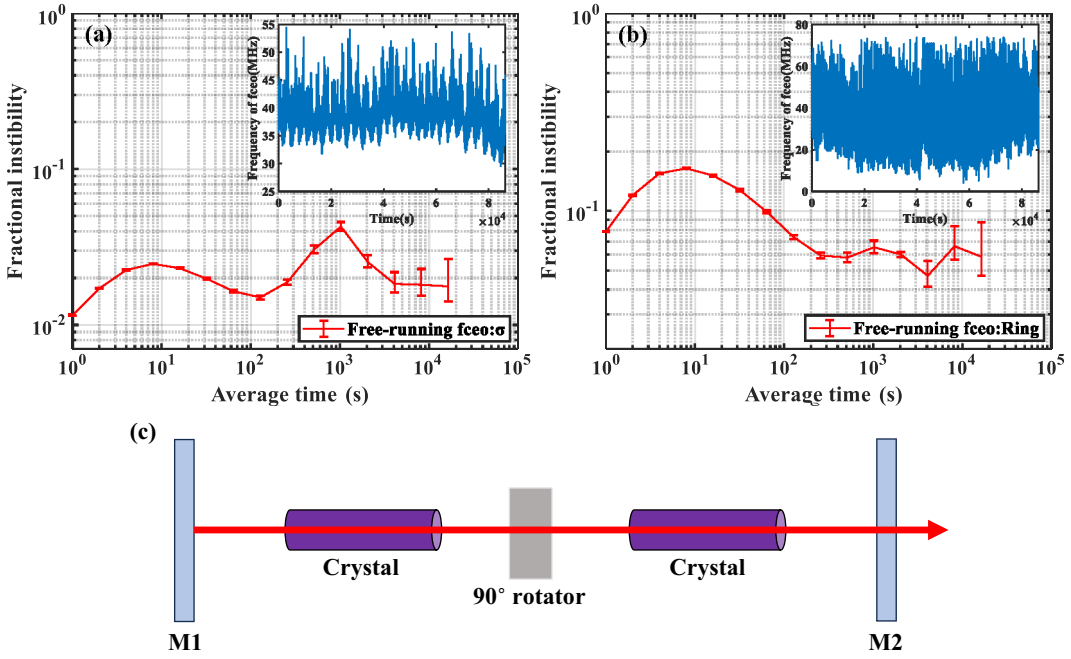


Fig. 5. Overlapping Allan deviations of the free-running f_{ceo} for (a) σ cavity and (b) ring cavity. Insets: free-running f_{ceo}. (c) Schematic diagram of thermal birefringence compensation.[27]

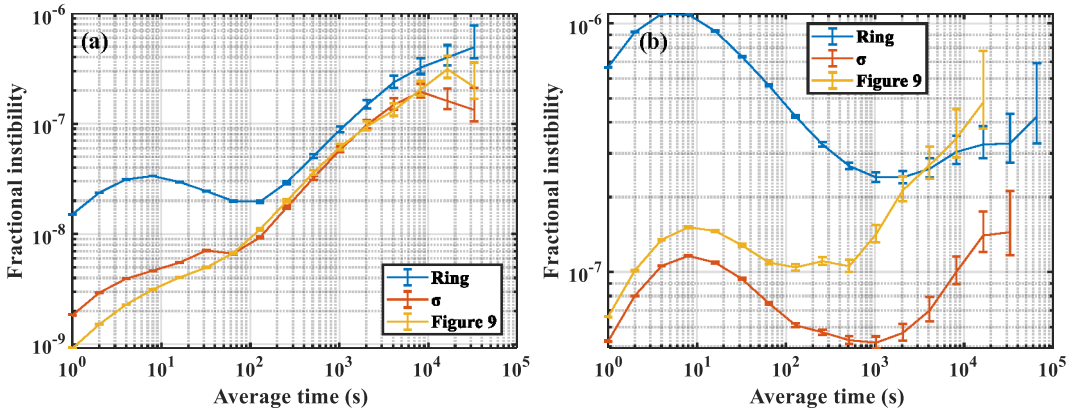


Fig. 6. Overlapping Allan deviations of the ring cavity, σ cavity, and Figure-9 cavity in the closed (a) and open (b) states of the box.

As shown in Fig. 5, we also used a counter to measure the free-running carrier–envelope offset frequency (f_{ceo}) of combs generated from both the σ cavity and the ring cavity (the other two lasers had nearly identical parameters to the σ cavity and the ring cavity described above). To demonstrate the environmental disturbance resistance of the laser, we kept the lids of the plastic boxes housing the two seed sources open during the measurement. Both in terms of frequency drift and the 1 s overlapping Allan deviation, the σ cavity structure exhibits relatively good stability. This may be due to the Faraday rotator and the mirror within the σ cavity rotating the polarization state, potentially giving rise to a compensation effect similar to the thermal birefringence compensation effect commonly observed in solid-state lasers,[27] as shown in Fig. 5(c). However, it cannot be excluded that the cavity structure, similar to the Figure-9 cavity itself, possesses a certain resistance to environmental disturbances.

We also evaluated the noise performance of the three lasers by monitoring their repetition frequencies over a period exceeding 24 h, as shown in Fig. 6.

The unlocked repetition rate is susceptible to variations caused by environmental factors such as temperature and vibration. When a mode-locked laser is enclosed in a plastic box, the repetition rate stability of the ring cavity, σ cavity, and Figure-9 cavity over a 1 s averaging time is 1.5×10^{-8}, 1.8×10^{-9}, and 9.2×10^{-10}, respectively. In addition, when the box is opened, the 1 s average repetition frequency stability of the σ cavity is of the same order of magnitude as that of the Figure-9 cavity, and is better than that of the ring cavity.

To verify that differences between PM and non-PM fibers have minimal impact on the results, we conducted a comparative experiment under both stable and suboptimal environmental conditions. The above results were all measured on a laboratory optical platform, which provides a relatively stable environment. Next, we measured the noise under less favorable conditions. Due to other work constraints, the σ cavity was inconvenient to move, so we used it as a control group and measured its noise on the laboratory optical platform. The ring cavity and the Figure-9 cavity (another laser with nearly identical parameters to the Figure-9 laser described above) were placed on a small mobile support platform for noise measurement, making them more susceptible to vibrational and other environmental disturbances. The experiment used a Thorlabs 1015 driver to drive another laser diode, and the phase noise was measured with an EOT ET-3000A. The results are shown in Table 3.

The results show that the σ cavity, when placed on the laboratory optical platform, exhibits only slight differences in phase noise due to minor environmental changes or measurement errors. However, the ring cavity and the Figure-9 cavity, when placed on a small mobile support platform, are significantly affected by environmental vibrations and noise. Compared with the results obtained when placed on the experimental platform, the integrated timing jitter from 1 Hz to 1 kHz changed by 14183 fs and 3819 fs, respectively. This indicates that polarization-maintaining (PM) fibers do indeed reduce environmental interference to some extent, while the phase noise of lasers based on non-polarization-maintaining fibers is strongly affected. However, when all three cavity-type structures are placed on a laboratory optical platform and enclosed in protective plastic boxes, the 4644 fs integrated timing jitter difference between the σ cavity and the ring cavity with similar fiber is much smaller than the 19955 fs difference observed in poorer environments. This suggests that a more stable testing environment can mitigate the impact of environmental interference on non-PM fibers. Furthermore, in a stable environment, the σ cavity does not show a significant difference compared with the Figure-9 cavity using polarization-maintaining fiber. Moreover, in Fig. 6(b), with the box open, the repetition-rate stability at an averaging time of 1 s was comparable between the σ cavity and the Figure-9 cavity.

Table 3. Integrated Timing Jitter from 1 Hz to 1 kHz in Stable and unstable environments.

	σ	Ring	Figure-9
Stable environment	11852 fs	16496 fs	7675 fs
Poor environment	10723 fs	30679 fs	11494 fs

4. Discussion

This paper focuses on low-noise seed sources for optical frequency combs and studies the impact of cavity structures on the noise of mode-locked lasers. We made our best efforts to ensure consistency across all factors other than the cavity configuration. The Figure-9 cavity achieved excellent performance with integrated timing jitter of 107 fs (10 Hz–10 kHz) and integrated RIN of 0.0037% (1 Hz–1 MHz). Notably, the σ cavity, which shares a similar structural design with the Figure-9 cavity, also demonstrated a degree of noise suppression capability.

Acknowledgment

Project supported by the Scientific Research Foundation of National Institute of Metrology, China (Grant Nos. AKYZD2411 and AKYZD2511).

References

[1] Picqué N and Hänsch T W 2019 *Nat. Photonics* **13** 146
[2] Shao X, Han H, Yan Y, Ma J, Li C and Wei Z 2024 *Appl. Phys. Lett.* **124** 171103
[3] Leopardi H, Davila-Rodriguez J, Quinlan F, Olson J, Sherman J A, Diddams S A and Fortier T M 2017 *Optica* **4** 879

[4] Yang M Z, Meng F, Lin Y G, Song Y J, Fang Z J and Hu M L 2020 *Laser Optoelectron. Prog.* **57** 181
[5] Herman D I, Walsh M, Kreider M K, Lordi N, Tsao E J, Lind A J, Heyrich M, Combes J, Genest J and Diddams S A 2025 *Science* **387** 653
[6] Newbury N R, Coddington I and Swann W 2010 *Opt. Express* **18** 7929
[7] Wan Z, Chen Y, Zhang X, Yan M and Zeng H 2025 *Light Sci. Appl.* **14** 257
[8] Shao X D, Han H N and Wei Z Y 2021 *Acta Opt. Sin.* **70** 134
[9] Yan L L, Ruan J, Zhang P, Rao B J, Li M K, Du Z J and Zhang S G 2025 *Photonics* **12** 153
[10] Kim J and Song Y J 2016 *Adv. Opt. Photonics* **8** 465
[11] Newbury N R and Swann W C 2007 *J. Opt. Soc. Am. B* **24** 1756
[12] Han H N and Wei Z Y 2016 *Physics* **45** 449
[13] He J, Hu J, Ouyang D, Tang Z, Luo X, Wang J, Dong F, Yan P, Wang J, Guo C and Ruan S 2024 *Infrared Phys. Technol.* **142** 105550
[14] Kim T K, Song Y J, Jung K, Kim C, Kim H, Nam C H and Kim J 2011 *Opt. Lett.* **36** 4443
[15] Mayer A S, Grosinger W, Fellinger J, Winkler G, Perner L W, Droste S, Salman S H, Li C, Heyl C M, Hartl I and Heckl O H 2020 *Opt. Express* **28** 18946
[16] Song Y J, Kim C, Jung K, Kim H and Kim J 2011 *Opt. Express* **19** 14518
[17] Li X, Zou W W and Chen J P 2015 *Electron. Lett.* **51** 351
[18] Hänsel W, Hoogland H, Giunta M, Schmid S, Steinmetz T, Doubek R, Mayer P, Dobner S, Cleff C, Fischer M and Holzwarth R 2017 *Appl. Phys. B* **123** 41
[19] Wang L D, Zhang Y Y, Rao B J, Jiang H F and Zhang S G 2019 *J. Time Freq.* **42** 1
[20] Chen J, Sickler J W, Ippen E P and Kärtner F X 2007 *Opt. Lett.* **32** 1566
[21] Han Y, Tian H C, Meng F, Wang K and Cao S Y 2022 *Opt. Express* **30** 48021
[22] Li M K, Yang X G, Rao B J, Yan L L, Chen X, Yuan R, Zhang P, Zhang Y Y and Liu T 2023 *Front. Phys.* **11** 1044842
[23] Novak S and Moesle A 2002 *J. Lightwave Technol.* **20** 975
[24] Zhao J, Guiraud G, Floissat F, Gouhier B, Rota-Rodrigo S, Traynor N and Santarelli G 2017 *Opt. Express* **25** 357
[25] Jung K and Kim J 2015 *Opt. Lett.* **40** 316
[26] Tian H C, Raabe N, Song Y J, Steinmeyer G and Hu M L 2018 *Opt. Lett.* **43** 3108
[27] Moshe I and Jackel S 2002 *Opt. Commun.* **214** 315